

Superconducting phase coherence in the presence of a pseudogap: Relation to specific heat, tunneling and vortex core spectroscopies

Qijin Chen[†] and K. Levin

James Franck Institute, University of Chicago, Chicago, Illinois 60637

Ioan Kosztin

Beckman Institute and Department of Physics, University of Illinois, Urbana, IL 61801

(October 31, 2018)

In this paper we demonstrate how, using a natural generalization of BCS theory, superconducting phase coherence manifests itself in phase insensitive measurements — when there is a smooth evolution of the excitation gap Δ from above to below T_c . In this context, we address the underdoped cuprates. Our premise is that just as Fermi liquid theory is failing above T_c , BCS theory is failing below. The order parameter Δ_{sc} is different from the excitation gap Δ . Equivalently there is a (pseudo)gap in the excitation spectrum above T_c which is also present in the underlying normal state of the superconducting phase. A central emphasis of our paper is that the latter gap is most directly inferred from specific heat and vortex core experiments. At the same time there are indications that fermionic quasiparticles exist below T_c so that many features of BCS theory are clearly present. A natural reconciliation of these observations is to modify BCS theory slightly without abandoning it altogether. Here we review such a modification based on a BCS-like ground state wavefunction. A central parameter of our extended BCS theory is $\Delta^2 - \Delta_{sc}^2$ which is a measure of the number of bosonic pair excitations which have a non-zero net momentum. These bosons are present in addition to the usual fermionic quasiparticles. Applying this theory we find that the Bose condensation of Cooper pairs, which is reflected in Δ_{sc} , leads to sharp peaks in the spectral function once $T \leq T_c$. These are manifested in ARPES spectra as well as in specific heat jumps, which become more like the behavior in a λ transition as the pseudogap develops. We end with a discussion of tunneling experiments and condensation energy issues. Comparison between theoretical and experimental plots of C_v , and of tunneling and vortex core spectroscopy measurements is good.

PACS numbers: 74.20.-z, 74.20.Fg, 74.25.Bt, 74.25.Fy

I. INTRODUCTION

In the underdoped regime of high temperature superconductors it is now clear that Fermi liquid theory is failing and the “smoking gun” for this failure is a (pseudo)gap in fermionic excitation spectrum above T_c . Many would argue^{1,2} that this failure is evidence for spin-charge separation. However, the fact that the excitation gap evolves smoothly into its counterpart in the superconducting phase may also be interpreted as evidence for “preformed pairs”. In this way superconducting pairing correlations are responsible for the breakdown of the Fermi liquid state. This picture appears rather natural in view of the notably short coherence length ξ in these materials, which leads to a breakdown of the strict mean field theory of BCS. Within this short ξ scheme, one considers that pairs form at temperature T^* and Bose condense at lower temperature T_c . These are not true “preformed” or bound pairs but rather long lived³⁻⁵ pair states. Many have argued for this viewpoint from experimentalists⁶⁻¹⁰ to theorists.^{11,12}

Our contribution¹³⁻¹⁷ to this body of work has been to show how to microscopically implement this preformed pair approach at all temperatures $T \leq T_c$, by deriving an extension of BCS theory, based on the ground state of Leggett.¹⁸ We have also addressed³⁻⁵ the behavior above T_c . In this extended BCS approach, the fermionic excitation gap Δ (which evolves smoothly from above to below T_c ^{19,20}) and the mean field order parameter Δ_{sc} (which is non-vanishing below T_c)

are not necessarily the same at any non-zero temperature; this is a reflection of the distinction between T^* and T_c . Since $\Delta \neq \Delta_{sc}$, we say that there are pseudogap effects below T_c . *The normal state underlying the superconducting phase is not a Fermi liquid.* The excitations of the system can be viewed as a “soup” of fermions and pairs of fermions (bosons). The latter are very long-lived at and below T_c in the long wave-length limit; their number is associated with the difference $\Delta^2 - \Delta_{sc}^2$.

This background sets the stage for the important questions which we address in this paper. What are the signatures of T_c , in thermodynamical quantities such as the specific heat, C_v , given the smooth evolution of the excitation gap? How do we understand the abrupt appearance of long lived, fermionic “quasiparticles” below T_c , and their implications for the electronic spectral function $A(\mathbf{k}, \omega)$? If the superconducting state is not Fermi-liquid based, then how does one extrapolate the “normal state” below T_c in order to deduce such thermodynamical properties as the condensation energy?

One of the central observations underlying this paper is the fact that there are two distinct experiments which provide seemingly similar information about the extrapolated normal state, i.e., that this $T \leq T_c$ state contains an excitation gap. These are scanning tunneling microscopy (STM) data in a vortex core^{8,21} as well as specific heat measurements.²² Renner and co-workers⁸ have argued that their vortex experiments “show either the presence of important superconducting fluctuations or preformed pairs”. Loram²²⁻²⁴ and co-workers have analyzed their specific heat data to show that a ther-

modynamically consistent picture of C_v reflects a gap in the ($T \leq T_c$) “normal” state spectrum, not directly related to the condensate. This would, they argue, include the possibility of preformed pairs that retained their structure below T_c , as in He⁴, and whose binding energy does not contribute to the condensation energy. Alternative explanations for the vortex core experiments have been advanced by Franz and Millis,²⁵ and more recently by Franz and Tesanovic²⁶ and by Lee and Wen.²⁷

This “preformed pair” picture, which is essentially a mean field-based approach, should be contrasted with the phase fluctuation picture of Emery and Kivelson²⁸ which has been implemented by Franz and Millis²⁵ to address photoemission and tunneling spectroscopies. In the present case the normal state excitations represent a “soup” of fermions and bosons, whereas in the approach of Ref. 25 the system is thought to consist of a soup of fluctuating vortices. It is widely believed that, at least below T_c , fermionic quasiparticles are present so that the phase fluctuation picture will eventually need to accommodate their contributions. Loram²⁴ has, moreover, argued that phase fluctuations are not consistent with the behavior of C_v , which he observes.

The results which we obtain in this paper show that upon entering the superconducting phase, the onset of the coherent condensate, characterized by Δ_{sc} , leads to a sharpening of the peaks in the electronic spectral function, which will be directly reflected in ARPES studies where its effects are quite dramatic, as well as in tunneling.²⁹ ARPES measurements support such a peak sharpening, and it has been recently claimed,³⁰ as is consistent with the theme of this paper, that the observed sharpening at T_c (rather than at T^*) is difficult to understand within strict BCS theory.

Indeed, BCS theory can and should be generalized, and in its more general form, this peak sharpening in conjunction with the temperature dependence of the excitation gap, is also responsible for a specific heat jump. The latter, is thus, quite generally, associated with the onset of off-diagonal long range order. When this general picture is applied to the cuprates we find that in the overdoped regime, this jump (in C_v) can be quantified in terms of the temperature dependence of the excitation gap Δ (as in the traditional BCS case, see Eq. 18 below). This is in contrast to the underdoped regime, where the order parameter and excitation gap are distinct and where the excitation gap is smooth across T_c . Here the jump (associated only with Δ_{sc}) becomes smaller towards underdoping, where the pseudogap is more prominent. Moreover, the shape of the C_v versus T curve is more like the λ transition of Bose-Einstein condensation (BEC). All of these features seem to be consistent with experiment.^{24,6}

An important second theme of this paper is an analysis of the extrapolated normal state below T_c . We argue here that the superconductivity is non-Fermi liquid based and that this has important implications for condensation energy estimates. Moreover, the non-Fermi liquid characteristics of the extrapolated normal state (which underlies the superconducting phase) should help provide constraints on the long standing controversy² of Fermi liquid break-down in the normal state. Indeed, spin-charge separation scenarios^{27,26} might be

distinguishable from alternatives such as the present one, or that of Ref. 25 by studies *below* T_c . This provides a major impetus for the present work.

II. THEORETICAL FRAMEWORK

A. Overview

Our work begins with the ground state wavefunction of BCS as generalized by Leggett¹⁸

$$\Psi_0 = \Pi_{\mathbf{k}}(u_{\mathbf{k}} + v_{\mathbf{k}}c_{\mathbf{k}\uparrow}^\dagger c_{-\mathbf{k}\downarrow}^\dagger)|0\rangle \quad (1)$$

which describes the continuous evolution between a BCS system, having weak coupling g and large ξ , towards a BEC system with large g and small ξ . Here $u_{\mathbf{k}}, v_{\mathbf{k}}$, which are defined as in BCS theory, are self consistently determined in conjunction with the number constraint. *The central approximation of this paper is the choice of this ground state wavefunction.* The essence of our previous contributions^{13,16,17} has been a characterization of the excitations of Ψ_0 and their experimental signatures (for all $T \leq T_c$). New thermodynamical effects stemming from bosonic degrees of freedom must necessarily enter, as one crosses out of the BCS regime, towards Bose-Einstein condensation.

As in BCS theory, we presume that there exists some attractive interaction between fermions of unspecified origin which is written as $V_{\mathbf{k},\mathbf{k}'} = g\varphi_{\mathbf{k}}\varphi_{\mathbf{k}'}$, where $g < 0$; here, $\varphi_{\mathbf{k}} = 1$ and $(\cos k_x - \cos k_y)$ for s - and d -wave pairing, respectively. The fermions are assumed to have dispersion, $\epsilon_{\mathbf{k}} = 2t_{\parallel}(2 - \cos k_x - \cos k_y) + 2t_{\perp}(1 - \cos k_{\perp}) - \mu$, measured with respect to the fermionic chemical potential μ . Here t_{\parallel} and t_{\perp} are the in-plane and out-of-plane hopping integrals, respectively. In a quasi-two dimensional (2D) system, $t_{\perp} \ll t_{\parallel}$. For brevity, we use a four momentum notation $K \equiv (\mathbf{k}, i\omega)$, $\sum_K \equiv T \sum_{\mathbf{k},\omega}$, etc., and suppress $\varphi_{\mathbf{k}}$ until the final equations.

We now make a number of important observations about BCS theory. BCS theory involves a special form for the pair susceptibility $\chi(Q) = \sum_K G(K)G_0(Q - K)$, where the Green's function G satisfies $G^{-1} = G_0^{-1} + \Sigma$, with $\Sigma(K) = -\Delta_{sc}^2 G_0(-K)$. In this notation, the gap equation is

$$1 + g\chi(0) = 0, \quad T \leq T_c. \quad (2)$$

As was first observed by Kadanoff and Martin,³¹ this BCS gap equation can be rederived by truncating the equations of motion so that only the one (G) and two particle (\mathcal{T}) propagators appeared. Here G depends on Σ which in turn depends on \mathcal{T} . In general \mathcal{T} has two additive contributions,¹³ from the condensate (sc) and the non-condensed (pg) pairs. Similarly the associated self energy³¹

$$\Sigma(K) = \sum_Q \mathcal{T}(Q)G_0(Q - K) \quad (3)$$

can be decomposed into $\Sigma_{pg}(K) + \Sigma_{sc}(K)$. The two contributions in Σ come respectively from the condensate, $\mathcal{T}_{sc}(Q) = -\Delta_{sc}^2 \delta(Q)/T$, and from the $Q \neq 0$ pairs, with $\mathcal{T}_{pg}(Q) = g/(1 + g\chi(Q))$.

More generally, at larger g , the above equations hold but we now include feedback into Eq. (2) from the finite momentum pairs, via $\Sigma_{pg}(K) = \sum_Q \mathcal{T}_{pg}(Q) G_0(Q - K) \approx G_0(-K) \sum_Q \mathcal{T}_{pg}(Q) \equiv -\Delta_{pg}^2 G_0(-K)$, which defines a pseudogap parameter, Δ_{pg} . This last approximation is valid only because (through Eq. (2)), \mathcal{T}_{pg} diverges as $Q \rightarrow 0$. In this way, $\Sigma_{pg}(K)$ has a BCS-like form, as does the total self energy $\Sigma(K) = -\Delta^2 G_0(-K)$, where

$$\Delta^2 = \Delta_{sc}^2 + \Delta_{pg}^2. \quad (4)$$

For the physically relevant regime of moderate g , we have found, after detailed numerical calculations,^{15,16} that \mathcal{T}_{pg} may be approximated as

$$\mathcal{T}_{pg}^{-1}(\mathbf{q}, \Omega) = a_0(\Omega - \Omega_{\mathbf{q}} + \mu_{pair} + i\Gamma_{\mathbf{q}}). \quad (5)$$

where the pair dispersion $\Omega_{\mathbf{q}} = q^2/2M_{pair}$ and the effective pair chemical potential $\mu_{pair} = 0$ for $T \leq T_c$. The effective pair mass M_{pair} and the coefficient a_0 are determined via a Taylor expansion¹⁷ of \mathcal{T}_{pg}^{-1} . Moreover, $\Gamma_{\mathbf{q}} \rightarrow 0$, as $\mathbf{q} \rightarrow 0$. As a consequence we have

$$\Delta_{pg}^2 = - \sum_Q \mathcal{T}_{pg}(Q) = \frac{1}{a_0} \sum_{\mathbf{q} \neq 0} b(\Omega_{\mathbf{q}}). \quad (6)$$

We now rewrite Eq. (2), along with the fermion number constraint, as

$$1 + g \sum_{\mathbf{k}} \frac{1 - 2f(E_{\mathbf{k}})}{2E_{\mathbf{k}}} \varphi_{\mathbf{k}}^2 = 0, \quad (7)$$

$$\sum_{\mathbf{k}} \left[1 - \frac{\epsilon_{\mathbf{k}}}{E_{\mathbf{k}}} + \frac{2\epsilon_{\mathbf{k}}}{E_{\mathbf{k}}} f(E_{\mathbf{k}}) \right] = n \quad (8)$$

Here $f(x)$ and $b(x)$ are the Fermi and Bose functions and $E_{\mathbf{k}} = \sqrt{\epsilon_{\mathbf{k}}^2 + \Delta^2 \varphi_{\mathbf{k}}^2}$ is the quasiparticle dispersion.

Equations (6)-(8) represent the central equations of our theory below T_c . They are consistent with BCS theory at small g , and with the ground state Ψ_0 at all g ; in both cases the right hand side of Eq. (6) is zero. The simplest physical interpretation of the present decoupling scheme is that it goes beyond the standard BCS mean field treatment of the single particles (which also acquire a self energy from the finite \mathbf{q} pairs), but it *treats the pairs at a self consistent mean field level*.

III. SPECTRAL FUNCTIONS, DENSITIES OF STATES AND SPECIFIC HEAT

Experimentally, it has been established from specific heat measurements in the cuprates that there is a step discontinuity or a maximum at T_c , depending on the doping level.^{23,24} It is clear that one cannot explain these experiments using the standard picture of BCS theory, in which the specific heat jump at

T_c results from the opening of the excitation gap. We now address these experiments. In Section II, we used an approximate form for the pseudogap self-energy Σ_{pg} (see derivation of Eq. (4)), in order to simplify the calculations. Under this approximation, Σ_{pg} has a BCS-like character, so that the spectral function is given by two δ -functions at $\pm E_{\mathbf{k}}$. These approximations were justified in the context of the applications considered, thus far.¹³⁻¹⁷

However, in order to study quantities which rely on details of the density of states, we will, in the remainder of this paper, relax this simplifying approximation and allow for lifetime effects in Σ_{pg} . This more realistic form for Σ_{pg} incorporates a finite broadening γ due to the incoherent nature of the finite center-of-mass momentum pair excitations. In this way we distinguish this contribution from that of the condensate. To make numerical calculations tractable,^{4,5} we do not solve for the broadening γ and excitation gap Δ self-consistently. This would involve an iterative solution of the complex set of three coupled equations for G and \mathcal{T} ; rather we take Δ below T_c from Eqs. (6)-(8), and use our estimates^{4,5} of T^* to determine where pseudogap effects are essentially negligible. More importantly, we treat the broadening as a phenomenological parameter, with one adjustable coefficient, chosen to optimize fits to tunneling experiments. Our results, throughout this paper, are not particularly sensitive to the detailed form of γ (which will depend on doping concentration x and T),³² but it is essential that γ be non-zero and appreciable when compared with T . In this same spirit, we take T_c , and the chemical potential μ from our leading order calculations (with $\gamma=0$).

We turn now to the spectral function $A(\mathbf{k}, \omega)$. It follows from our microscopic scheme that slightly above^{4,5} T_c , and for all $T \leq T_c$,¹³ the self energy associated with the $\mathbf{q} \neq 0$ pairs, and that from the condensate or $\mathbf{q} = 0$ pairs is given respectively by

$$\Sigma_{pg}(\mathbf{k}, \omega) = \frac{\Delta_{\mathbf{k},pg}^2}{\omega + \epsilon_{\mathbf{k}} + i\gamma} - i\Sigma_0(\mathbf{k}, \omega), \quad (9)$$

and

$$\Sigma_{sc}(\mathbf{k}, \omega) = \frac{\Delta_{\mathbf{k},sc}^2}{\omega + \epsilon_{\mathbf{k}}}, \quad (10)$$

where $\Delta_{\mathbf{k},pg} = \Delta_{pg} \varphi_{\mathbf{k}}$ and $\Delta_{\mathbf{k},sc} = \Delta_{sc} \varphi_{\mathbf{k}}$. Here we have added to Σ_{pg} an additional piece Σ_0 which is not accounted for by our (particle-particle) ladder diagrams. This leads to an ‘‘incoherent’’ background contribution which we will address later in the context of the cuprates. For the rest of the discussion in the next two sections we set $\Sigma_0 = 0$ and, thereby, focus only on the superconducting and pseudogap terms.

The spectral function can readily be computed from $\Sigma = \Sigma_{sc} + \Sigma_{pg}$, as

$$A(\mathbf{k}, \omega) = -2 \text{Im} G(\mathbf{k}, \omega + i0), \quad (11)$$

which satisfies the sum rule $\int_{-\infty}^{\infty} \frac{d\omega}{2\pi} A(\mathbf{k}, \omega) = 1$. We, thus, obtain a relatively simple expression for $A(\mathbf{k}, \omega)$ which applies below and above T_c , respectively:

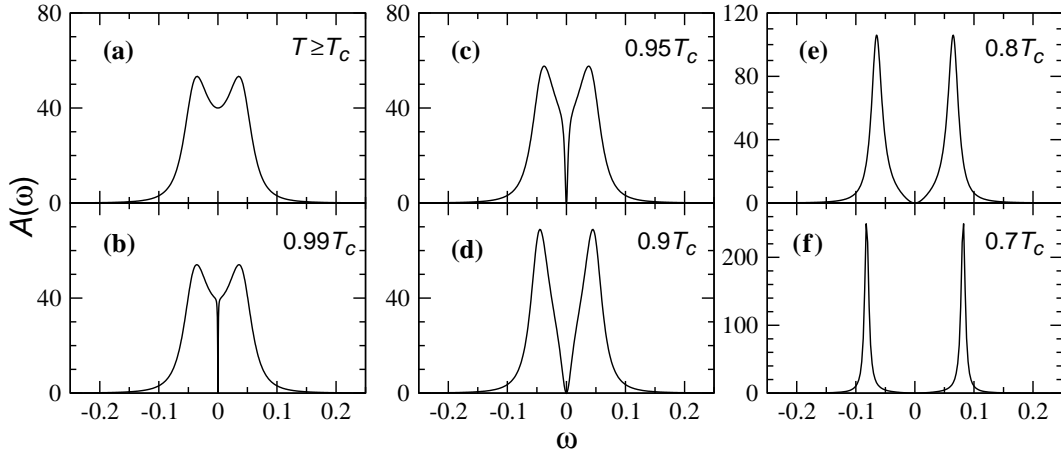


FIG. 1. Behavior of the coherent contribution to the spectral function at various T , for wavevectors away from the nodes.

$$A(\mathbf{k}, \omega) = \frac{2\Delta_{\mathbf{k},pg}^2 \gamma (\omega + \epsilon_{\mathbf{k}})^2}{(\omega + \epsilon_{\mathbf{k}})^2 (\omega^2 - E_{\mathbf{k}}^2)^2 + \gamma^2 (\omega^2 - \epsilon_{\mathbf{k}}^2 - \Delta_{\mathbf{k},sc}^2)^2}, \quad (12a)$$

$$A(\mathbf{k}, \omega) = \frac{2\Delta_{\mathbf{k}}^2 \gamma}{(\omega^2 - E_{\mathbf{k}}^2)^2 + \gamma^2 (\omega - \epsilon_{\mathbf{k}})^2}, \quad (12b)$$

From Eq. (12a), we see that the spectral function contains a zero at $\omega = -\epsilon_{\mathbf{k}}$ below T_c , whereas it has no zero above T_c . This difference is responsible for the different thermodynamical behavior across T_c .

In Fig. 1, we plot the spectral function for $\epsilon_{\mathbf{k}} = 0$ (on the Fermi surface) at different temperatures from slightly above T_c [Fig. 1(a)] to temperatures within the superconducting phase [Fig. 1(f)]. This figure is typical of situations in which there is a well established pseudogap. The figure can be viewed as representative of both s - and d -wave order parameter symmetries. Hence the value of the wave-vector \hat{k} is not particularly relevant, provided it is away from the nodal points in the d -wave case. For illustrative purposes, we take \hat{k} at the anti-nodes, with $\gamma(T) = \Delta_{pg}(T_c)$, and $\Delta_{pg}(T_c) = 0.05$ (in units of $4t_{\parallel}$). In this way we ignore any T dependence in γ and, thus, single out the long range order effects associated with Δ_{sc} .

These figures give the first clear indications of the onset of “quasiparticle” coherence. Moreover, panel (a) helps to emphasize an important component of our physical picture: the superconductor is not in a Fermi liquid state just above T_c , as can be seen by the non-Fermi liquid form for the spectral function. Just below T_c , the dramatic dip at $0.99T_c$ is a consequence of Bose condensation of $\mathbf{q} = 0$ pairs. Here, a very small condensate contribution nevertheless leads to the depletion of the spectral weight at the Fermi level, as shown in Fig. 1(b). As the temperature continues to decrease, and the superconducting gap increases, the two peaks in the spectral function become increasingly well separated, as plotted in Figs. 1(c)-(f). Even at the relatively high temperatures corresponding to $T/T_c \sim 0.7$, the spectral peaks are quite sharp — only slightly broadened relative to their BCS counterparts (where the spectral function is composed of two δ functions).

It should be stressed that lifetime effects via γ do not lead to significant peak broadening. This follows from the fact that the imaginary part of the pseudogap self-energy at the peak location $E_{\mathbf{k}}$ is given by (for $\epsilon_{\mathbf{k}} = 0$)

$$\gamma' = \gamma \frac{\Delta_{\mathbf{k},pg}^2}{(E_{\mathbf{k}} + |\epsilon_{\mathbf{k}}|)^2 + \gamma^2} = \gamma \frac{\Delta_{\mathbf{k},pg}^2}{\Delta_{\mathbf{k}}^2 + \gamma^2}. \quad (13)$$

Since Eq. (6) indicates that Δ_{pg} vanishes as $T \rightarrow 0$, the effective peak width, determined by γ' , decreases with decreasing T . It can be seen that below T_c , the spectral function in Eq. (12b), is very different from that obtained using a simple broadened BCS form; there is no true gap for the latter, in contrast to the present case.

These spectral functions can be used to derive the density of states (per spin) as

$$N(\omega) = \sum_{\mathbf{k}} A(\mathbf{k}, \omega). \quad (14)$$

Moreover, it is expected that peak sharpening effects discussed above for the spectral function are also reflected in the density of states. For simplicity, we first consider the case of s -wave pairing. In Fig. 2(a)-(f), the density of states is plotted for a quasi-2D s -wave superconductor, where the various energy gaps are taken to be the same as in Fig. 1. Because of contributions from states with $\epsilon_{\mathbf{k}} \neq 0$, the narrow dips in Fig. 1(b)-(c) do not show up here. However, as is evident, the density of states within the gap region decreases quickly, as the superconducting condensate develops.

The rapid decrease of the density of states with decreasing T , in the vicinity of T_c , will be reflected in the behavior of the specific heat, C_v and, thereby, lead to the thermodynamical signature of the phase transition. C_v may be obtained from $C_v = dE/dT$, where the energy E is calculated via:³³

$$E = 2T \sum_{\mathbf{k}, n} \frac{1}{2} (i\omega_n + \epsilon_{\mathbf{k}}^0 + \mu) G(\mathbf{k}, i\omega_n) \\ = \sum_{\mathbf{k}} \int_{-\infty}^{\infty} \frac{d\omega}{2\pi} (\omega + \epsilon_{\mathbf{k}} + 2\mu) A(\mathbf{k}, \omega) f(\omega), \quad (15)$$

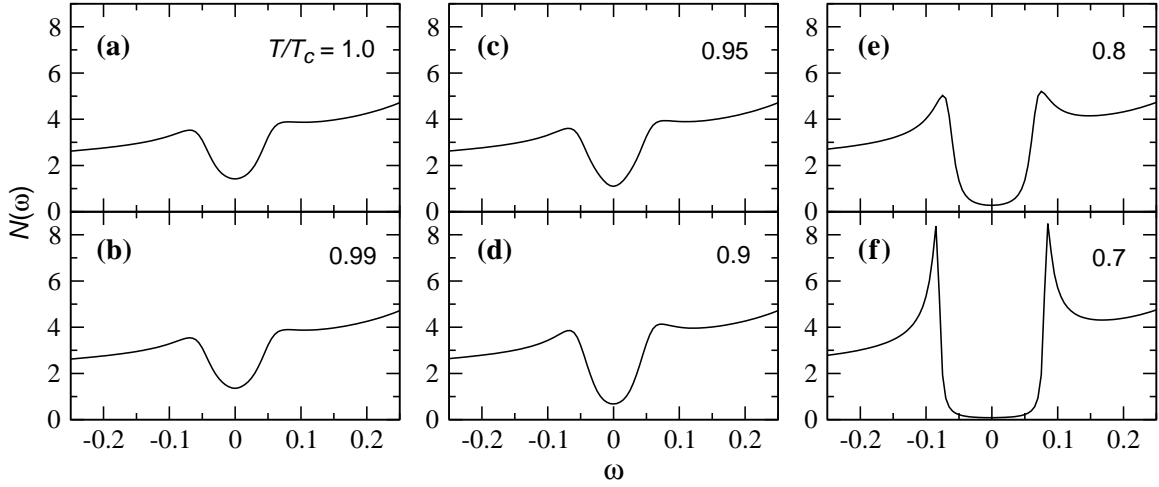


FIG. 2. Effects of superconducting long range order on the behavior of the density of states as a function of temperature in a pseudogapped s -wave superconductor with $n = 0.5$. Here we take the parameters to be the same as those used in Fig. 1. At $T/T_c \sim 0.7$, as shown in (f), the density of states is close to that of strict BCS theory.

where $\epsilon_{\mathbf{k}}^0 = \epsilon_{\mathbf{k}} + \mu$ is the dispersion measured from the bottom of the band. It follows that

$$E = \int_{-\infty}^{\infty} \frac{d\omega}{2\pi} [(\omega + \mu)N(\omega) + K(\omega)]f(\omega), \quad (16)$$

where we have defined $K(\omega) \equiv \sum_{\mathbf{k}} \epsilon_{\mathbf{k}}^0 A(\mathbf{k}, \omega)$, which can be regarded as the contribution associated with the kinetic energy of the system. In this way, we obtain

$$C_v = \int_{-\infty}^{\infty} \frac{d\omega}{2\pi} \left\{ \frac{\partial \mu}{\partial T} N(\omega) f(\omega) - [(\omega + \mu)N(\omega) + K(\omega)] \frac{\omega}{T} f'(\omega) + \left[(\omega + \mu) \frac{\partial N(\omega)}{\partial T} + \frac{\partial K(\omega)}{\partial T} \right] f(\omega) \right\}. \quad (17)$$

The first two terms on the right hand side lead to a “normal metal-like” contribution to C_v/T which is proportional to $N(\omega)$ at low T . However, the third term arises because $N(\omega)$ depends on T . In this case, C_v/T no longer reflects the density of states. It is this term that will give rise to the specific heat discontinuity at T_c .

In Fig. 3 we plot the temperature dependence of C_v in both (a) the weak coupling BCS case and (b) the moderate coupling pseudogap case with s -wave pairing. We choose, for definiteness, the broadening $\gamma(T) = T$ for the second of these calculations. We also indicate in the insets, the respective temperature dependent excitation gaps, which have been assumed^{13,16} in producing the figure.

In both cases shown in Fig. 3, the specific heat jump arises from a discontinuity in $dN(\omega)/dT$,³⁴ associated with the onset of superconducting order. However, for the BCS case, this derivative can be associated with a discontinuity in the derivative of the excitation gap, via

$$\Delta C_v^{BCS} = -N(0) \frac{d\Delta^2}{dT}. \quad (18)$$

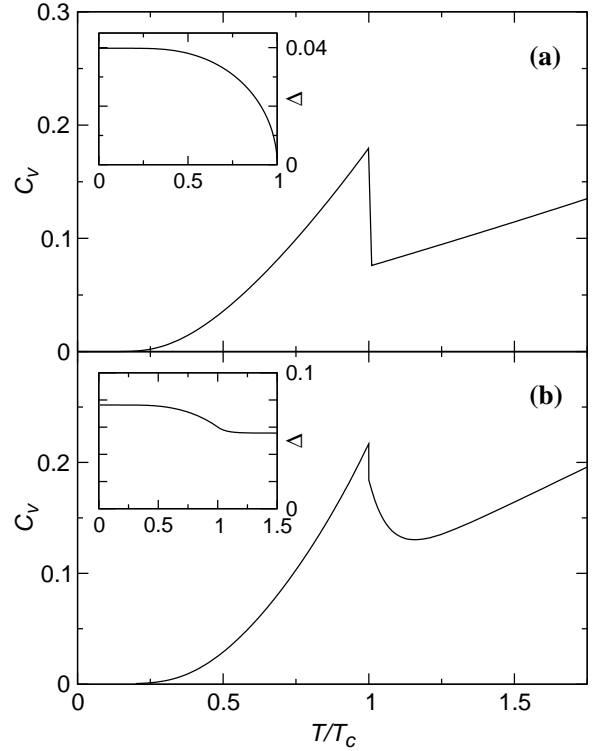


FIG. 3. Comparison of the temperature dependence of the specific heat in the (a) weak coupling BCS case and (b) moderate coupling pseudogap case. Shown here are quasi-2D s -wave results, at $n = 0.5$, $-g/4t_{\parallel} = 0.5$ and 0.6 , respectively. The T dependence of the gap is shown as insets.

By contrast, in the pseudogap case, the gap Δ and its derivative $d\Delta/dT$ are presumed to be continuous across T_c as shown in the inset to Fig. 3(b), and in Fig. 4 below, so that Eq. (18) does not hold. Moreover, in this case, above but near T_c , the temperature dependence in the density of states is still impor-

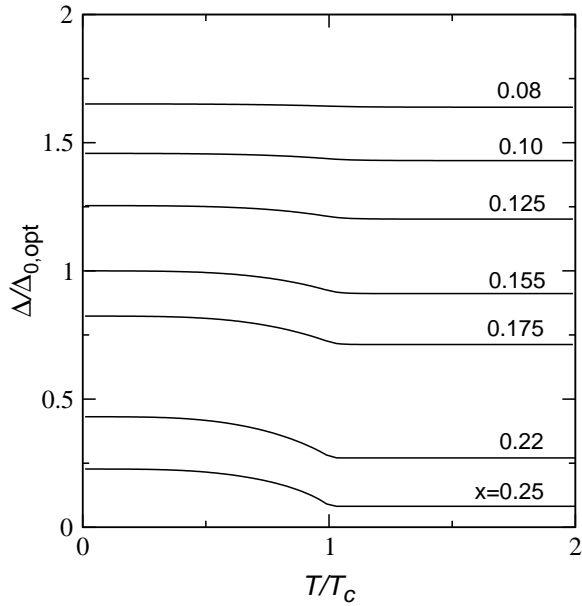


FIG. 4. Temperature dependence of the excitation gaps for various doping concentrations used for calculations in Fig. 6. Here $\Delta_{0,opt}$ is the zero T gap at optimal doping $x \approx 0.15$.

tant due to the presence of an excitation gap above T_c . The latter leads to a decrease in $dN(\omega)/dT$ which is then reflected³⁵ in a decrease in C_v , slightly above T_c . At higher T , well away from T_c , where $dN(\omega)/dT$ tends gradually to zero, C_v is then controlled, as in a more typical “normal metal”, by $N(\omega)$. We see, then, that the approach to the “normal metal” value is sharp for BCS, but because of the non-zero pseudogap, it is more gradual for case (b). An important consequence of these effects, is that the shape of the anomaly in C_v (shown in Fig. 3(b)) is more characteristic of a λ -like transition, although there is a precise step function discontinuity just at T_c .

IV. APPLICATION TO THE CUPRATES

The results obtained in Sec. III are generally valid for both s - and d -wave cases, and can be readily applied to the d -wave cuprates. In this section we test the physical picture and the results obtained above, by studying the tunneling spectra and the specific heat behavior in the cuprates, as a function of doping and of temperature. As in earlier work,^{16,17} we introduce a hole concentration dependence of the electronic energy scales by imposing the Mott constraint that the in-plane hopping integral $t_{||}(x) = t_0 x$, so that the plasma frequency vanishes as $x \rightarrow 0$. As a result, the effective coupling strength $-g/t_{||}(x)$ increases as the Mott insulator phase is approached. Here we assume (for simplicity) $g(x) = g$ and fit the one free parameter g/t_0 to the phase diagram.¹⁶

In order to compare with tunneling spectra, we introduce a slightly more realistic band structure which includes a next-nearest neighbor hopping term, $-2t'(1 - \cos k_x \cos k_y)$, in the band dispersion, $\epsilon_{\mathbf{k}}$, with $t'/t_{||} \approx 0.4$. This parameter choice gives rise to the hole-like Fermi surface shape seen in ARPES

measurements for under- and optimally doped cuprates,^{36,37} and places the van Hove singularity in a more correct position within the band.

Finally, we turn to the phenomenological parameter γ as well as to Δ . We presume that γ changes from above to below T_c and in this way Δ (which is directly coupled to γ via the set of coupled equations for G and \mathcal{T}) will have some, albeit small, structure in its temperature dependence at T_c , as seems to be the case experimentally. Our choice for the excitation gaps is shown in Fig. 4, and appears compatible with Figs. 8 and 9 in Ref. 22. As is consistent with scattering rate measurements in the literature,^{38,39} we take $\gamma \propto T^3$ below T_c and linear in T above T_c .⁴⁰ For the doping dependence, we assume that γ varies inversely with Δ . This reflects the fact that when the gap is large, the available quasiparticle scattering decreases. With these reasonable assumptions, along with the continuity of γ at T_c , we obtain a simple form:

$$\gamma = \begin{cases} aT^3/T_c\Delta, & (T < T_c), \\ aTT_c/\Delta, & (T > T_c). \end{cases} \quad (19)$$

Here, the coefficient $a \leq 1$. This corresponds to our single adjustable parameter.

A. Tunneling spectra

Tunneling experiments were among the first to provide information about the excitation gap — which measurements seem to be consistent with ARPES data.⁹ For a given density of states $N(\omega)$, the quasiparticle tunneling current across a superconducting-insulator-normal (SIN) junction can be readily calculated,⁴¹

$$I_{SIN} = 2eN_0T_0^2 \int_{-\infty}^{\infty} \frac{d\omega}{2\pi} N(\omega) [f(\omega - eV) - f(\omega)], \quad (20)$$

where we have assumed a constant density of states, N_0 , for the normal metal, and presumed that the tunneling matrix element T_0 is isotropic. In reality, there may be some directional tunneling which will tend to accentuate the gap features, but we do not complicate our discussion here with these effects. At low T , one obtains

$$\left(\frac{dI}{dV} \right)_{SIN} \approx \frac{e^2 N_0 T_0^2}{\pi} N(eV) \quad (21)$$

so that the tunneling spectra and the density of states are equivalent, up to a multiplicative constant coefficient. At T comparable to T_c , however, the tunneling spectra reflect a more thermally broadened density of states.

In Fig. 5(a), we plot the SIN tunneling spectra, calculated for optimal doping ($x \approx 0.15$) at temperatures varying from above to below T_c . The van Hove singularity introduces a broad maximum in the spectra at high temperatures, as seen for the top curve in Fig. 5(a). We see here that (even for this optimal sample), as observed experimentally,⁹ the density of states contains (pseudo)gap like features which lead to two peaks. This is visible for temperatures well above T_c . A

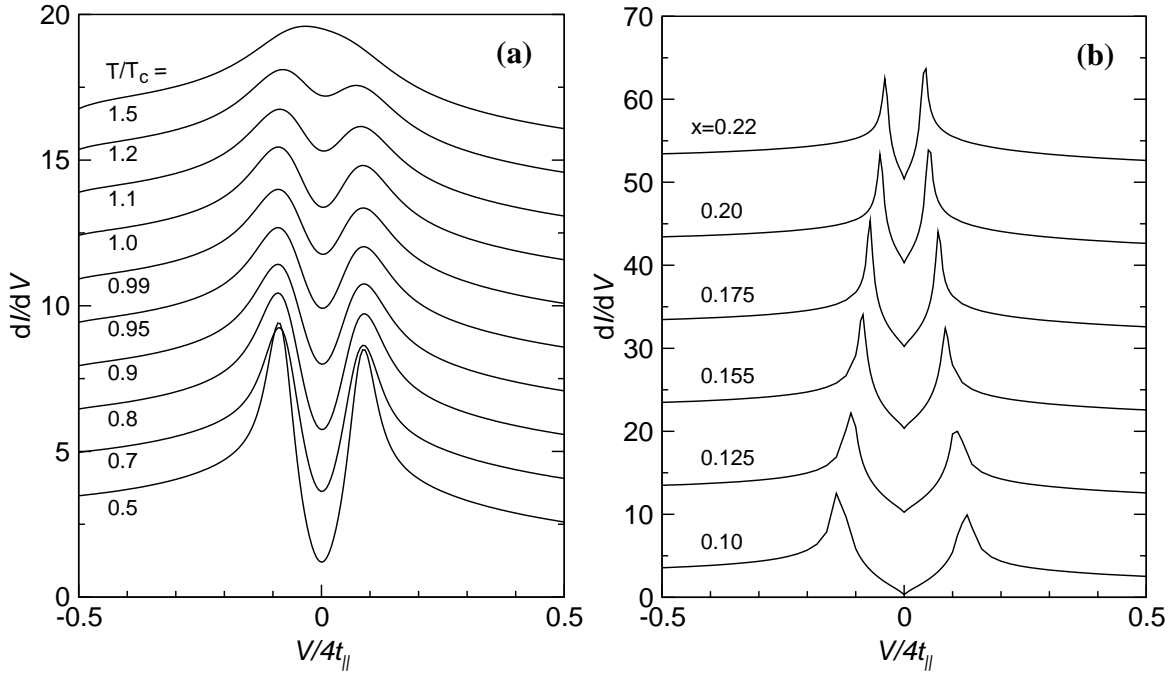


FIG. 5. (a) Temperature and (b) doping dependence of tunneling spectra across an SIN junction. Shown in (a) are the dI/dV characteristics calculated for optimal doping at various temperatures from above to below T_c . Shown in (b) are tunneling spectra at low T (at $0.2T_c$) for various x . The units for dI/dV are $e^2 N_0 T_0^2 / 4t_{||}$, where $t_{||}$ is evaluated at optimal doping. For clarity, the curves in (a) and (b) are vertically offset by 1.5 and 10, respectively.

similar plot is presented in Fig. 5(b), which shows at fixed low $T = 0.2T_c$ how the spectrum evolves as a function of x . Both these plots appear in reasonable agreement with what is observed experimentally by Renner and coworkers⁴² and by Miyakawa *et al*⁴³ for $\text{Bi}_2\text{Sr}_2\text{CaCu}_2\text{O}_{8+\delta}$ (Bi2212).

B. Specific heat

There is a substantial amount of experimental data on the specific heat in the cuprates,^{24,6} although systematic studies come primarily from one experimental group.²⁴ We compare our numerical results with these data by plotting our calculations for C_v/T in Fig. 6(a)-(f), from over- to underdoped systems. As shown in these plots, the behavior of C_v is BCS-like in the overdoped regime. As the system passes from optimal doping towards underdoping, the behavior is more representative of a λ -like anomaly, as found in Fig. 3(b) for the s -wave case. All these trends seem to be qualitatively consistent with experimental data.^{23,24} In the underdoped regime at high T , we find a maximum in C_v/T , near a temperature, T^* , which may be associated with the onset of the pseudogap state [See, e.g, Fig. 7(c)]. Finally, in contrast to Fig. 3, at low T , the d -wave nodes lead to a larger quasiparticle specific heat, than for the s -wave case.

The experimentally observed λ -like anomaly of C_v at T_c has been interpreted previously as evidence for a Bose condensation description.⁶ Here, in contrast, we see that within our generalized mean field theory, this anomaly naturally

arises from the temperature dependence of the fermionic excitation gap which has some structure at, but persists above, T_c , as shown in Fig. 4. Thus, this is a property of superconductors which have a well established pseudogap. That the experimental data, (which, except at extremely reduced hole concentrations), show a reasonably sharp (λ -like) structure at T_c — seems to reinforce the general theme of this work — that corrections to BCS theory may be reasonably accounted for by an improved mean field theory, rather than by, say, including order parameter fluctuation effects.

V. LOW T EXTRAPOLATION OF THE PSEUDOGAPPED NORMAL STATE

A. Non-Fermi liquid based superconductivity

The character of the extrapolated ($T \leq T_c$) “normal state” is at the core of many topical issues in high T_c superconductivity. Understanding this state may shed light on the nature of Fermi liquid break-down above T_c . Moreover, the thermodynamics of this extrapolated phase provide a basis for estimates of the condensation energy. This is deduced²⁴ by integrating the difference between the entropy of the superconducting state and that of the extrapolated normal state with respect to T . This extrapolated normal state also appears as a component of the free energy functional of conventional Landau-Ginzburg theory. Indeed, considerable attention has been paid recently to the condensation energy in the context

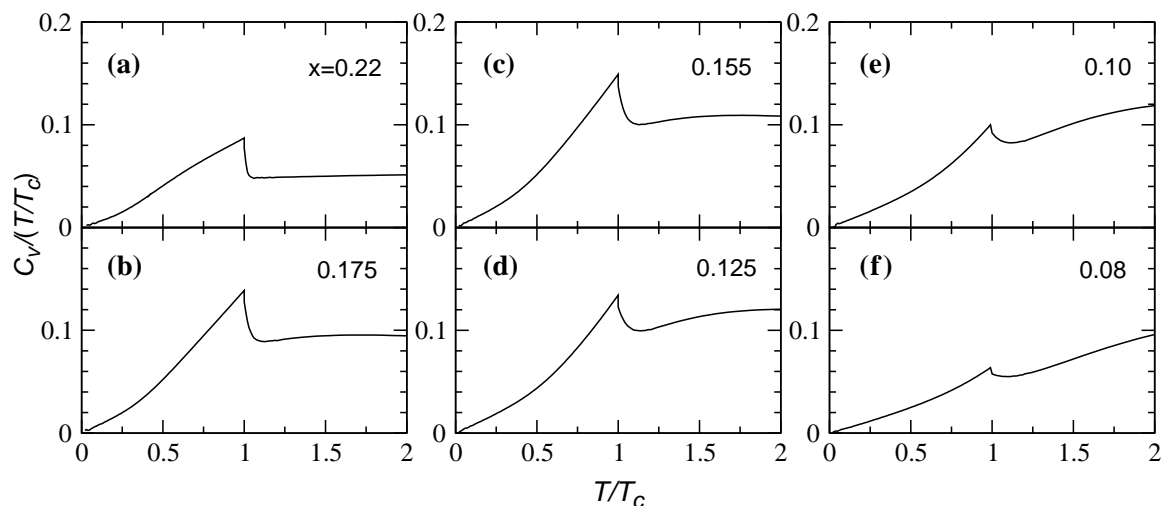


FIG. 6. Temperature dependence of the specific heat for various doping concentrations, calculated with $a = 1/4$ in Eq. 19.

of determining the pairing “mechanism” in the high temperature superconductors.^{44–46} In this regard what is needed is the difference between the various “normal” and superconducting state polarizabilities (e.g., magnetic and electric) which are thought to be responsible for the pairing. It is important to stress that *the “normal state” used in computing the polarizabilities should contain an excitation gap which is compatible with that found in the experimental data analysis²⁴ with which the microscopically deduced condensation energy is compared.*

We have emphasized that within our physical picture there is an underlying (pseudo)gap in the normal state below T_c . A similar picture was independently deduced phenomenologically from specific heat and magnetic susceptibility measurements by Loram and co-workers²² who arrived at equations like those of Section II [Eqs. (4) and (7)]. However, they did not impose a self consistent condition on Δ_{pg} as in Eq. (6). Rather the quantity Δ_{pg} (which they call E_g) is assumed to be T -independent.

To expand on these issues we plot in Fig. 7 the calculated C_v/T and entropy S for (a)-(b) the BCS case, as compared with the counterparts obtained for the pseudogap superconductor in (c) and (d). The dotted lines represent the Fermi liquid, i.e., linear extrapolation (FL). Figures 7(a) and (b) reaffirm that this Fermi liquid extrapolation is sensible for the BCS case — C_v/T is a constant, and S is a straight line going through the origin. Panel (b) is useful in another respect: it shows how the entropy behaves as phase coherence is established. In general, the phase coherent state has a lower entropy than the extrapolated normal state.

In the underdoped regime, Loram and co-workers²⁴ have stressed that entropy measurements lead one to infer that an excitation gap occurs *above* T_c . We analyze our calculated form of the entropy in a similar fashion. In contrast to the BCS case, for a pseudogap superconductor, the Fermi liquid extrapolation of S is unphysical, approaching a negative value at low T , as shown by the dotted line in Fig. 7(d). Here the solid and dotted lines separate around the temperature T^* which we

find to be around $1.5T_c$. In order to obtain a thermodynamically consistent picture, then, the normal state must deviate from the FL line and this is accomplished by turning on an excitation gap at $T \leq T^*$.

The dashed lines in Fig. 7(c)-(d) show a more reasonable extrapolated normal state (labelled PG) which is equivalent to the solid line for $T \geq T_c$ and distinct for $T < T_c$. This extrapolation is taken to be consistent with the conservation of entropy, $S = \int_0^T C_v/T dT$, i.e., the shaded areas in (c) and (d). This construction for the $T \leq T_c$ normal state, is similar to the procedure followed experimentally,²⁴ and, in effect, removes phase coherent contributions which enter via Δ_{sc} . This construction is by no means unique; all that is required is that the entropy of the extrapolated normal and of the superconducting states be equal at $T = T_c$. As shown in the figure, we chose, for simplicity, a straight line extrapolation for C_v/T . Moreover, this choice is consistent with our expectation that there would be, in the “normal state”, a finite intercept for C_v/T .

Just as a gap is present above T_c , the underlying normal phase below T_c (labelled PG) is to be distinguished from the FL extrapolation; it also contains an excitation gap. Indeed, this is consistent with what has been claimed experimentally:²⁴ *a thermodynamically consistent picture of C_v reflects a gap in the $T \leq T_c$ normal state spectrum, not directly related to the condensate.* While Figs. 7(c)-(d) are similar to what is in the data in underdoped cuprates, in our analysis the “normal” state C_v/T and S are linear and quadratic in T , respectively. Slightly different power laws have been assumed experimentally. A rough estimate of the condensation energy can be obtained from the integrated area between the solid line (for the superconducting state) and the dashed line (for the extrapolated normal state) in Fig. 7(d). It should also be noted that a more meaningful measure of the condensation energy is obtained by computing the magnetic field dependent Gibbs free energy. This is more complicated to implement both theoretically and experimentally.

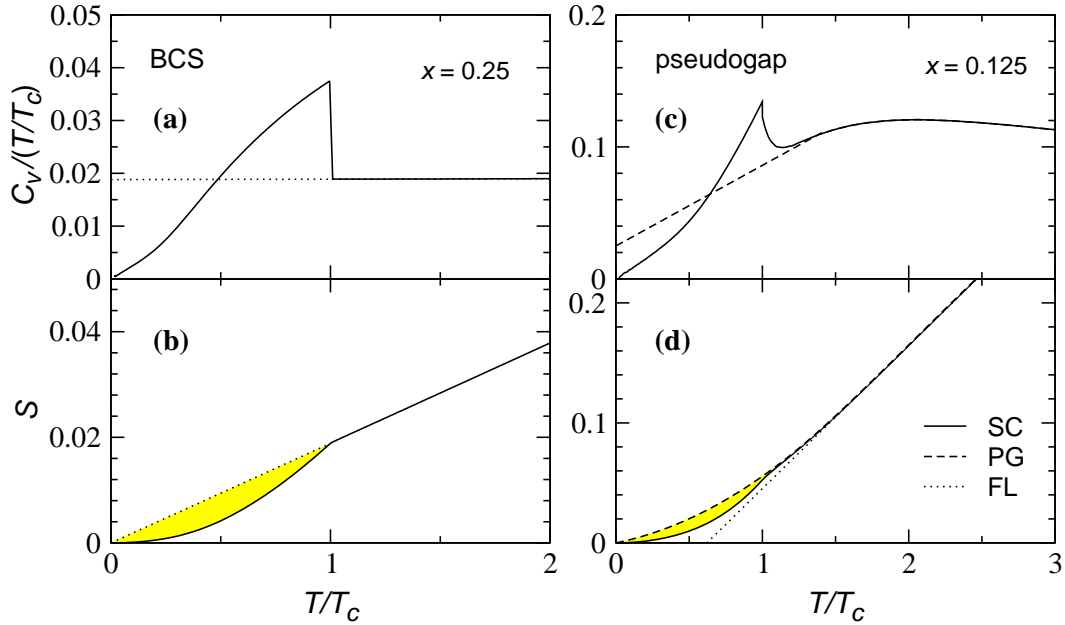


FIG. 7. Comparison of the extrapolated normal state below T_c in (a)-(b) BCS and (c)-(d) pseudogap superconductors. Shown are the extrapolations for C_v/T and the entropy S in the upper and lower panels, respectively. Here “SC”, “PG”, and “FL” denote superconducting state, extrapolated normal state with a pseudogap, and Fermi liquid based extrapolation, respectively. The shaded areas in (c) and (d) determine the condensation energy.

B. Comparison with vortex core and C_v measurements

The presence of a pseudogap in the underlying normal state of the superconducting phase is also consistent with the observations by Renner and co-workers⁸ based on STM measurements within a vortex core. While one might be concerned about magnetic field, H , effects in interpreting these data, it should be noted that H appears to have a rather weak effect⁴⁷ on pseudogap phenomena, as measured by T^* and $\Delta(H)$. [In more overdoped samples the field dependence becomes more apparent⁴⁸]. By contrast T_c is more sensitive to H .

Indeed, this weak dependence on H is often invoked in the literature as strong evidence against the “preformed” pair scenario. In the usual BCS case, pairs form precisely when phase coherence sets in. However, in the case of a pseudogap superconductor where the coupling is stronger, pairs form above T_c without an underlying phase coherence. It is clear that a magnetic field lowers T_c by destroying phase coherence. However, “preformed” pairs will survive H , leaving the excitation gap in tact. Stated alternatively, a magnetic field (just like magnetic impurities) breaks time reversal symmetry, and therefore makes it energetically unfavorable to form Cooper pairs which are comprised of time reversed single particle states. In contrast, finite momentum pair excitations, which are responsible for the pseudogap in our approach, are not formed in time reversed states, and as such, they are not as susceptible to external magnetic fields or to magnetic impurities.

In Fig. 8, we plot our results for the SIN tunneling characteristics, dI/dV , and the computed entropy and specific heat in a pseudogap superconductor, and compare with experiment.^{24,8,49} To obtain the extrapolated normal state

(called PG) in dI/dV , we set the superconducting order parameter Δ_{sc} to zero, but maintain the total excitation gap to be same as in a phase coherent, superconducting state — with non-zero Δ_{sc} (called SC). This procedure presumes that when the condensate is absent, the pseudogap Δ_{pg} must correspond to the full excitation gap. Thus it should reflect the pairs which would otherwise be condensed. The characteristic behavior of dI/dV measured in an SIN configuration is presented as a comparison between theory (left) and experiment (right) in the upper panels of Fig. 8. Here the experimental curves are taken from Ref. 8, measured for underdoped Bi2212 inside (PG) and outside (SC) a vortex core, respectively. The non-Fermi liquid nature of the extrapolated normal state can be clearly seen. In a similar fashion, we show the comparisons for the extrapolated entropy and specific heat between our theory and experiments of Ref. 24 for $Y_{0.8}Ca_{0.2}Ba_2Cu_3O_{7-\delta}$. Here $\gamma = C_v/T$. The agreement between the theoretically computed curves and experimentally deduced curves provides reasonable support for the present theoretical picture.

C. Discussion

In this section we re-visit some of the issues raised in this paper and in experiments on C_v , tunneling, vortex core and related spectroscopies. In contrast to what has been presented up until now, here we are more qualitative and, in some instances, more speculative.

*Intrinsic tunneling experiments.*⁵⁰ Considerable attention has been directed towards intrinsic tunneling experiments (in stacked layers), not only because they yield different results

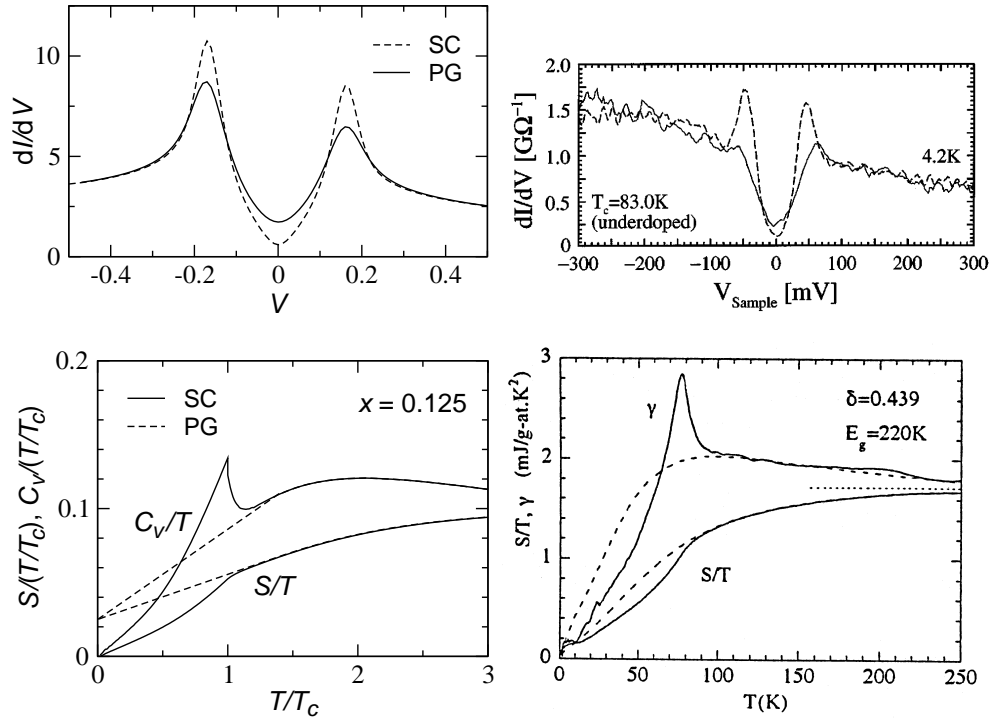


FIG. 8. Extrapolated normal state (PG) and superconducting state (SC) contributions to SIN tunneling and thermodynamics (left), as well as comparison with experiments (right) on tunneling for Bi2212 from Renner *et al.*⁸ and on specific heat for $Y_{0.8}Ca_{0.2}Ba_2Cu_3O_{7-\delta}$ from Loram *et al.*²⁴ The theoretical SIN curve is calculated for $T = T_c/2$, while the experimental curves are measured outside (dashed) and inside (solid) a vortex core.

from STM^{42,21} and from point contact/break junction⁴³ experiments, but also because they sometimes reveal an unexpected sharp feature (or second peak in dI/dV) presumably associated with superconductivity. This peak occurs in addition to a broader excitation gap feature (which is more like that found in single junction experiments) and it vanishes for $T \geq T_c$. There is, as yet, no complete convergence between different intrinsic Josephson junctions (IJJ) tunneling experiments. On overdoped samples Suzuki and co-workers⁵¹ have found anomalously sharp and large amplitude (second) peaks whose presence correlates with long range order, while, by contrast, Latyshev⁵² and co-workers find only a single maximum in dI/dV below T_c , which rather smoothly evolves into the normal state peak. However, for underdoped samples, Krasnov and co-workers⁵⁰ report two maxima below T_c , with a much less pronounced sharp feature than in Ref. 51, (although the latter appears to be descended from the more anomalous features reported earlier by Suzuki *et al.*). Earlier work⁵³ by some of his same co-authors found only a single gap feature, as was consistent with single junction data from other groups.^{43,8}

There is in all these experiments the possibility that the so-called superconducting peak is an artifact of self-heating or other non-equilibrium effects, which would be present when there is a non-zero critical current. Its absence in single junction experiments would, otherwise, be difficult to explain. These latter experiments correlate well with ARPES. Moreover, they also correlate with inferences from C_v and other

bulk data.^{54,9} We have no simple explanation for the sharp feature in tunneling. Within our approach there is a single excitation gap, Δ above as well as below T_c . Although the critical current¹⁶ I_c reflects the order parameter Δ_{sc} , which vanishes at T_c , this order parameter contribution is not expected to show up in quasiparticle tunneling as a second gap feature. Of these IJJ experiments, the data which seems not incompatible with our picture is that of Yurgens *et al.*,⁵³ and possibly Latyshev *et al.*;⁵² the latter authors, nevertheless, find much sharper maxima in dI/dV than we would have.

Quantum critical points: Both theorists⁵⁵ and experimentalists^{39,24} have recently turned their attention to quantum critical phase transitions. Moreover, these phenomena are assumed to be related to pseudogap effects. Indeed, Loram and co-workers²⁴ presume that Δ_{pg} (which, in their approach, is taken to be temperature independent) is proportional to T^* . Then at some critical doping concentration ($x \approx 0.19$), Δ_{pg} appears to vanish and they infer that $T^* \rightarrow 0$. By contrast, we find Δ_{pg} is more closely associated with $(T^* - T_c)$, which does not lead to a zero temperature phase transition, even when Δ_{pg} vanishes.

At low x , on the other hand, there may be something more dramatic like a first order or quantum critical phase transition going on — at the superconductor-insulator boundary. Here the excitation gap is maximum on one side of the boundary and yet the superconducting order parameter disappears on the other. [In the present picture this disappearance was found to arise from the localization of d -wave pairs¹⁵]. At

low x , this superconductor-insulator transition also appears in the presence of a magnetic field⁵⁶ when the field is large enough to drive the system into the normal phase. It also appears with impurity pair breaking.⁵⁷ All three of these experiments may be interpreted as suggesting that the fermionic excitation gap Δ survives in the presence of pair breaking (by large fields or impurities), or low hole concentrations — thereby leading to an insulating fermionic excitation spectrum. Some confirmation of this conjecture comes from NMR experiments⁴⁷ which seem to imply that Δ does not vary with H , once the pseudogap is well established. And the STM measurements,⁸ in general, as well as inside a vortex core seem consistent with the observation that Δ is only weakly H dependent. One cannot, of course, ignore Mott insulating effects at this superconductor-insulator boundary as well. However, whatever physical mechanism is dominant, the fact that the superconductor-insulator transition is a robust feature associated with the disappearance of superconductivity, whether by pair-breaking or by doping, needs to be addressed.

Incoherent contributions to the spectral function in photoemission:

Recent photoemission experiments^{58,30} indicate that the relative weight of the coherent contribution to the spectral function decreases rapidly with decreasing x . Ignoring the incoherent term Σ_0 in the self energy (as we have here) will necessarily affect any quantitative inferences about the systematic x dependence of the spectral function and, thereby, of C_v or the related condensation energy. This term can only be put in by hand in the present approach; it arises here from diagrams other than the particle-particle terms which give rise to the superconductivity and pseudogap. Moreover, the measured systematic x dependence of the coherent spectral weight, which has been inferred from photoemission,^{58,30} is likely to be consistent with the inferences based on thermodynamics²⁴ for the x dependence of the entropy S and related condensation energy. However, when the contribution from Σ_0 is sizeable, relative to the coherent terms, one cannot include it (by hand) without self-consistently also re-solving for the chemical potential μ and, hence, also for Δ and T_c , etc. This extensive numerical program would take us too far afield to implement here.

In addition, this Σ_0 contribution is needed to arrive at the well known⁵⁹ dip-hump features of photoemission. When this term is artificially added, we are able to obtain this latter structure which will scale with the excitation gap Δ . Indeed, a dependence on Δ is plausible since we presume that Σ_0 is associated with various (electron-hole) polarizabilities, which in the superconducting and pseudogap states reflect the non-vanishing excitation gap. It is, however, essential (to obtain dip-hump features) that the imaginary part of Σ_0 turns on rather abruptly at frequencies somewhere between Δ and 2Δ . Indeed, the step function model introduced in Ref. 60 seems to accomplish this quite well, but we know of no simple microscopic mechanism which yields this rapid frequency onset.

VI. CONCLUSIONS

This paper has raised some issues which have a number of important ramifications. We suggest that specific heat and vortex core experiments have provided strong evidence that the normal state underlying the superconducting phase is not a Fermi liquid. Thus BCS theory cannot be applied to the underdoped cuprates, without some modification. Since we have, as yet, very little alternative to BCS, it is natural first to try to extend it slightly. We believe the simplest and most benign modification is to adopt the Leggett extension of the ground state wavefunction, Eq. (1), (which is applicable to weak and strong coupling g) and extend his scheme to finite T . Within this approach we were able in the past to perform a number of concrete calculations,¹³⁻¹⁷ and, in the present paper, explore the behavior somewhat above and below T_c of the specific heat, C_v , and quasiparticle tunneling characteristics, dI/dV . This present study led us naturally to analyze the nature of superconducting phase coherence in the presence of a pseudogap.

Our study of C_v and dI/dV is based on a Green's function decoupling scheme chosen to be consistent with Eq. (1). The spectral functions which enter these two physical quantities depend, in turn, on the self energy which is the sum of Eqs. (9) and (10), where throughout we have ignored the incoherent term Σ_0 , which enters through diagrams other than those responsible for the superconducting and pseudo-gaps. It should be noted that this form for Σ is different from that introduced phenomenologically by Franz and Millis²⁵ and by Norman.⁶⁰ One of these groups,²⁵ in particular, emphasized the effects of the temperature dependent scattering rate. Here, by contrast, we emphasize the effects of long range phase coherence which sets in at T_c .

Because of the breakdown of BCS theory, in a superconductor with a pseudogap, the standard simplifications, such as Landau-Ginzburg expansions and Bogoliubov-de Gennes approaches²⁶ are not expected to hold, at least without some modifications. For the BCS case, the expansion in terms of a small order parameter which is identical to the excitation gap at T_c is possible. However, when the order parameter and the excitation gap are distinct as in the pseudogap case, there is no straightforward way to expand the free energy in terms of a small order parameter and to reflect the existence of a well established excitation gap simultaneously.

It should be emphasized, finally, that, in the non-BCS superconductor, there is an important distinction between T_c and the zero temperature excitation gap $\Delta(0)$. In the strong coupling, but still fermionic regime, as the pseudogap increases, T_c is suppressed.^{4,5,15} This observation allows us to respond to the widely repeated criticism of this “preformed” pair approach: namely that⁴⁷ “the gap is not closely tied to the onset of superconductivity” — as inferred from, say, the lack of magnetic field dependence in the former. Here we claim that in contrast to BCS theory, the excitation gap Δ is expected to be robust with respect to standard pair-breaking perturbations (such as magnetic fields and impurity scattering), while the order parameter, Δ_{sc} , is not. As emphasized throughout

this paper, the distinction between these two quantities is an essential component of the “preformed” pair approach.

This work was supported by the NSF-MRSEC, No. DMR-9808595 (QC and KL), and by the University of Illinois (IK). We thank A. V. Balatsky, K. E. Gray, Ying-Jer Kao, J. W. Loram, and J. F. Zasadzinski for helpful discussions.

† Current address: National High Magnetic Field Laboratory, 1800 E. Paul Dirac Dr., Tallahassee, Florida 32310

- ¹ P. A. Lee and X.-G. Wen, Phys. Rev. Lett. **78**, 4111 (1997).
- ² P. W. Anderson, *The Theory of Superconductivity in the High- T_c Cuprates* (Princeton University Press, Princeton, NJ, 1997).
- ³ B. Jankó, J. Maly, and K. Levin, Phys. Rev. B **56**, R11 407 (1997).
- ⁴ J. Maly, B. Jankó, and K. Levin, Physica C **321**, 113 (1999).
- ⁵ J. Maly, B. Jankó, and K. Levin, Phys. Rev. B **59**, 1354 (1999).
- ⁶ A. Junod, A. Erb, and Ch. Renner, Physica C **317-318**, 333 (1999).
- ⁷ Y. J. Uemura, Physica C **282-287**, 194 (1997).
- ⁸ Ch. Renner *et al.*, Phys. Rev. Lett. **80**, 3606 (1998).
- ⁹ T. Timusk and B. Statt, Rep. Prog. Physics **62**, 61 (1999).
- ¹⁰ G. Deutscher, Nature **397**, 410 (1999).
- ¹¹ M. Randeria, in *Bose Einstein Condensation*, edited by A. Griffin, D. Snoke, and S. Stringari (Cambridge Univ. Press, Cambridge, UK, 1995), pp. 355–92.
- ¹² P. Nozières and S. Schmitt-Rink, J. Low Temp. Phys. **59**, 195 (1985).
- ¹³ I. Kosztin, Q. J. Chen, B. Jankó, and K. Levin, Phys. Rev. B **58**, R5936 (1998).
- ¹⁴ I. Kosztin, Q. J. Chen, Y.-J. Kao, and K. Levin, Phys. Rev. B **61**, 11 662 (2000).
- ¹⁵ Q. J. Chen, I. Kosztin, B. Jankó, and K. Levin, Phys. Rev. B **59**, 7083 (1999).
- ¹⁶ Q. J. Chen, I. Kosztin, B. Jankó, and K. Levin, Phys. Rev. Lett. **81**, 4708 (1998).
- ¹⁷ Q. J. Chen, I. Kosztin, and K. Levin, Phys. Rev. Lett. **85**, 2801 (2000).
- ¹⁸ A. J. Leggett, in *Modern Trends in the Theory of Condensed Matter* (Springer-Verlag, Berlin, 1980), pp. 13–27.
- ¹⁹ H. Ding *et al.*, Nature **382**, 51 (1996).
- ²⁰ A. G. Loeser *et al.*, Science **273**, 325 (1996).
- ²¹ S. H. Pan *et al.*, cond-mat/0005484 (unpublished).
- ²² J. W. Loram *et al.*, J. Supercond. **7**, 243 (1994).
- ²³ J. W. Loram *et al.*, in *Proc. 10th Ann HTS workshop*, edited by B. Batlogg *et al.* (World Scientific, Singapore, 1996), pp. 341–344.
- ²⁴ J. W. Loram, K. A. Mirza, J. R. Cooper, and J. L. Tallon, J. Phys. Chem. Solids **59**, 2091 (1998).
- ²⁵ M. Franz and A. J. Millis, Phys. Rev. B **58**, 14 572 (1998).
- ²⁶ M. Franz and Z. Tesanovic, cond-mat/0002137 (unpublished).
- ²⁷ P. A. Lee and X.-G. Wen, cond-mat/0008419 (unpublished).
- ²⁸ V. J. Emery and S. A. Kivelson, Nature **374**, 434 (1995).
- ²⁹ We make a distinction here between tunneling and ARPES in the presence of an isotropic tunneling matrix element. For more directional tunneling, the difference between ARPES and tunneling experiments may be less apparent.
- ³⁰ D. L. Feng *et al.*, Science **289**, 277 (2000).
- ³¹ L. P. Kadanoff and P. C. Martin, Phys. Rev. **124**, 670 (1961).
- ³² For the *d*-wave case, we have also studied the effects associated with introducing a *k*-dependence in γ , and found that these effects are negligible.

³³ A. L. Fetter and J. D. Walecka, *Quantum Theory of Many-Particle Systems* (McGraw-Hill, San Francisco, 1971).

³⁴ Here by $dN(\omega)/dT$, we mean the Fermi function weighted average over a broad range of frequency. See the third term in Eq. 17.

³⁵ It should be emphasized that the temperature dependence of C_v at $T \gtrsim T_c$ is dominated by $dN(\omega)/dT$, instead of $N(\omega)$ itself. In fact the contributions of these two functions are in opposite directions as a function of temperature. This observation implies that one cannot extract the size of the excitation gap from the specific heat without taking proper account of the T dependence of the density of states. It should also be noted that the curvature above, but in the vicinity of T_c also reflects the subtle feature at T_c which appears in the excitation gap.

³⁶ H. Ding *et al.*, Phys. Rev. Lett. **78**, 2628 (1997).

³⁷ For this choice of t' , the van Hove singularities appear inside the filled lower half band. Because these effects were not particularly relevant in our previous studies, this complication was ignored previously.

³⁸ A. Hosseini *et al.*, Phys. Rev. B **60**, 1349 (1999).

³⁹ T. Valla *et al.*, Science **285**, 2110 (1999).

⁴⁰ Since the pseudogap equation (6) indicates $\Delta_{pg}^2 \propto T^{3/2}$ at low T , and Δ_{pg}^2 is roughly linear in T at $T \lesssim T_c$, this choice of $\gamma \propto T^3$ below T_c will give rise to a temperature dependence of the effective quasiparticle peak width $\gamma' \propto T^\alpha$ with $\alpha = 4 \sim 4.5$ for $T \leq T_c$, via Eq. (13). This is consistent with the experimentally observed $T^4 \sim T^5$ dependence of the quasiparticle scattering rate.³⁸ Above T_c , the T -dependence of Δ_{pg} is weak, so that $\gamma' \propto T$, in agreement with ARPES data.³⁹

⁴¹ G. D. Mahan, *Many-Particle Physics*, 2nd ed. (Plenum Press, New York, 1990).

⁴² Ch. Renner *et al.*, Phys. Rev. Lett. **80**, 149 (1998).

⁴³ N. Miyakawa, P. Guptasarma, J. F. Zasadzinski, D. G. Hinks, and K. E. Gray, Phys. Rev. Lett. **80**, 157 (1998); N. Miyakawa, J. F. Zasadzinski, L. Ozyuzer, P. Guptasarma, D. G. Hinks, C. Kendziora, and K. E. Gray, Phys. Rev. Lett. **83**, 1018 (1999).

⁴⁴ E. Demler and S.-C. Zhang, Nature **396**, 733 (1998).

⁴⁵ M. R. Norman, M. Randeria, B. Jankó, and J. C. Campuzano, Phys. Rev. B **61**, 14 742 (2000).

⁴⁶ A. J. Leggett, J. Phys. Chem. Solids **49**, 1729 (1998).

⁴⁷ K. Gorny *et al.*, Phys. Rev. Lett. **82**, 177 (1999).

⁴⁸ G. Zheng *et al.*, Phys. Rev. Lett. **85**, 405 (2000).

⁴⁹ In what follows we ignore the contribution from bound states to the core tunneling spectroscopy. Understanding these bound states will require a generalization of Bogoliubov-de Gennes theory for our extended BCS approach.

⁵⁰ V. M. Krasnov *et al.*, Phys. Rev. Lett. **84**, 5860 (2000).

⁵¹ M. Suzuki, T. Watanabe, and A. Matsuda, Phys. Rev. Lett. **82**, 5361 (1999).

⁵² Y. Latyshev *et al.*, cond-mat/0005116 (unpublished).

⁵³ A. Yurgens *et al.*, Int. J. Modern Phys. B **13**, 3758 (1999).

⁵⁴ J. L. Tallon and J. W. Loram, cond-mat/0005063 (unpublished).

⁵⁵ S. Chakravarty, R. B. Laughlin, D. K. Morr, and C. Nayak, cond-mat/0005443 (unpublished).

⁵⁶ Y. Ando *et al.*, Phys. Rev. Lett. **75**, 4662 (1995).

⁵⁷ Y. Zhao, H. K. Liu, G. Yang, and S. X. Dou, J. Phys. - Condens. Matter **5**, 3623 (1993).

⁵⁸ H. Ding *et al.*, cond-mat/0006143 (unpublished).

⁵⁹ M. R. Norman *et al.*, Phys. Rev. B **60**, 7585 (1999).

⁶⁰ M. R. Norman and H. Ding, Phys. Rev. B **57**, 11 089 (1998).